AKOYA BIOSCIENCES®
THE SPATIAL BIOLOGY COMPANY®

How Spatial Phenotyping Can Uncover Novel Insights in Tissue Biology

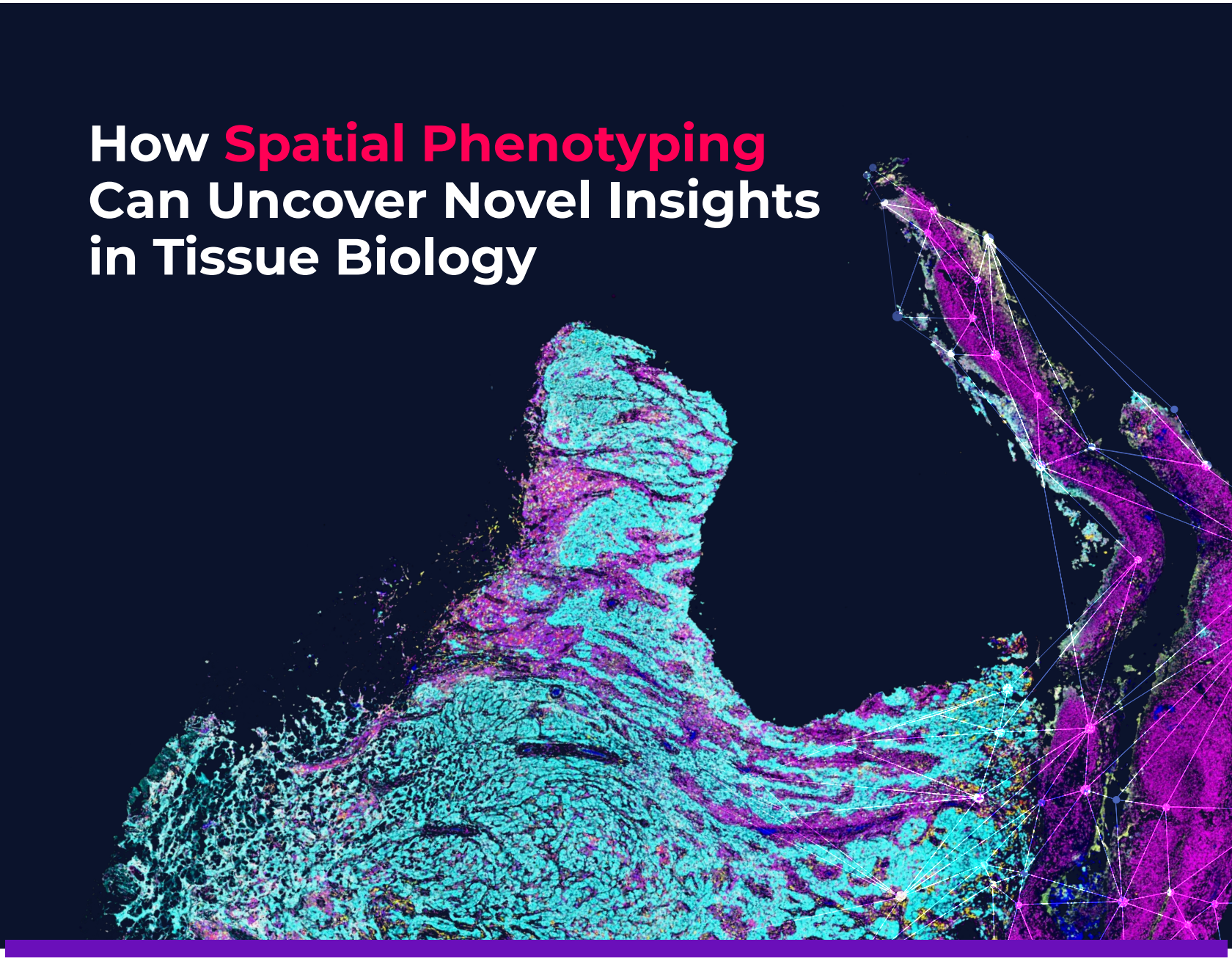

Spatial phenotyping allows a researcher to view, characterize, and quantify cells by lineage and variant with single-cell resolution in the context of an intact tissue sample. In areas such as oncology, immunology, and neurodegenerative disease it has opened new insights into the interplay between different cellular actors in promoting or suppressing disease.

For those not already employing spatial phenotyping in their labs, **this paper offers three examples of how it can impact your research tool kit.**

1 PUTTING CELLULAR FUNCTION IN CONTEXT

Call it biology's "uncertainty principle." With conventional analytical methods you are forced to choose between the detail of single-cell RNA-sequencing (scRNA-Seq), and the *in situ* capabilities of conventional immunohistochemistry (IHC). The former provides a flood of biomarker data but loses the context of the original sample, while the latter preserves the integrity of the tissue but restricts the analysis to a limited number of biomarkers.

Spatial phenotyping allows you to visualize and quantify dozens of biomarkers in a single tissue sample while maintaining cellular and sub-cellular detail. Shifting between different marker combinations on the same tissue section reveals unexpected patterns and associations that are not evident with other methodologies. It also allows you to see how the same cell types will behave differently based on their cellular microenvironments and identify distinct cellular clustering patterns prognosticative of outcomes. These "contextual phenotypes" based on adjacencies between cell types are providing researchers with new insights into inflammatory processes and tumor progression, and revealing novel targets for therapy.

> "You get all the information to characterize the cell while it's still intact within the tissue sample."

DR. KAI KESSENBROCK
Human Breast Cell Atlas Initiative, UC Irvine
https://www.akoyabio.com/hcawebinar

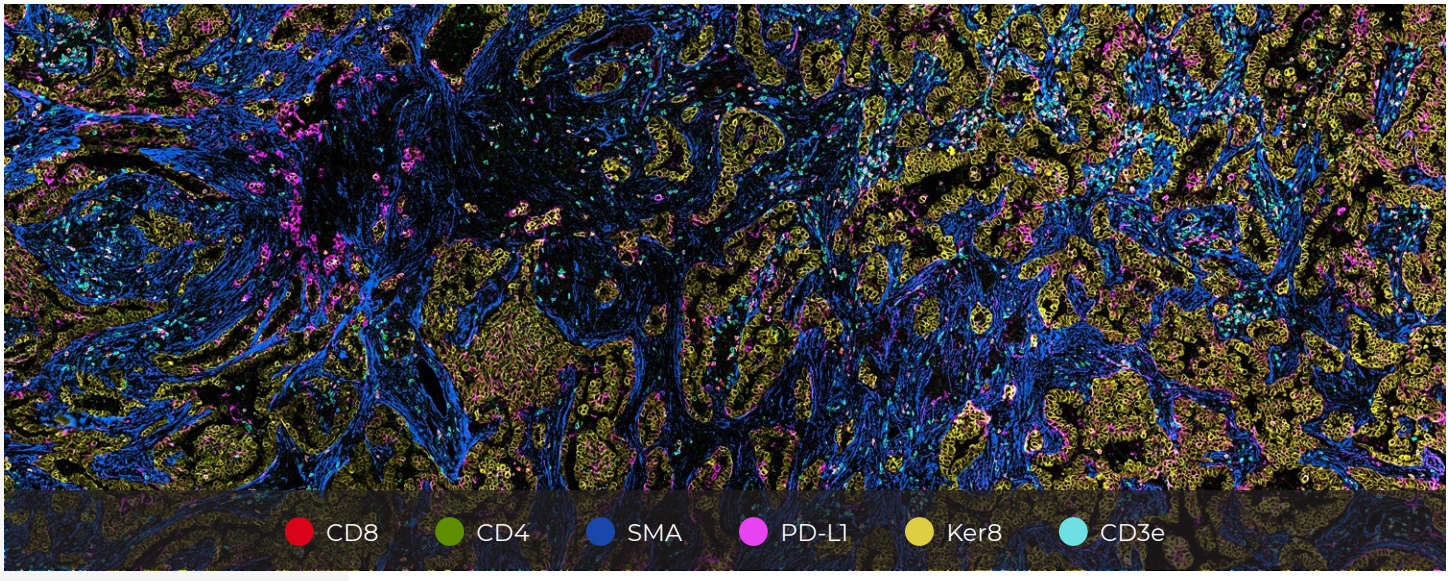

This is just one view of an FFPE sample of lung cancer tissue labeled with 39 different biomarkers. By looking at different expression levels, a researcher can identify the function and morphology of each cell, and distinguish different clustering patterns or "cellular neighborhoods" that are associated with different pathological findings.

In an example taken from Kessenbrock's work, **FIGURE 1** shows the result of a spatial phenotyping analysis of healthy breast tissue labeled with 34 different antibodies and containing more than 81,000 individual cells. By selecting for the nuclear marker DAPI, the epithelial marker Keratin-19, and the proliferation marker PCNA, we can clearly identify large lobular regions that contain secretory epithelial cells, as well as the narrow collecting ducts that eventually capture secreted fluids.

It is also worth noting what we do not see in **FIGURE 1**—the connective tissue, vimentin, lymphatic and fat cells that surround these lobular and ductal structures of interest. Those cells have been captured and can be visualized by selecting among the 30 other biomarkers applied to this sample, but because we are not limited to two or three markers, we have the flexibility to choose the images and analysis that best serve our analytical objectives.

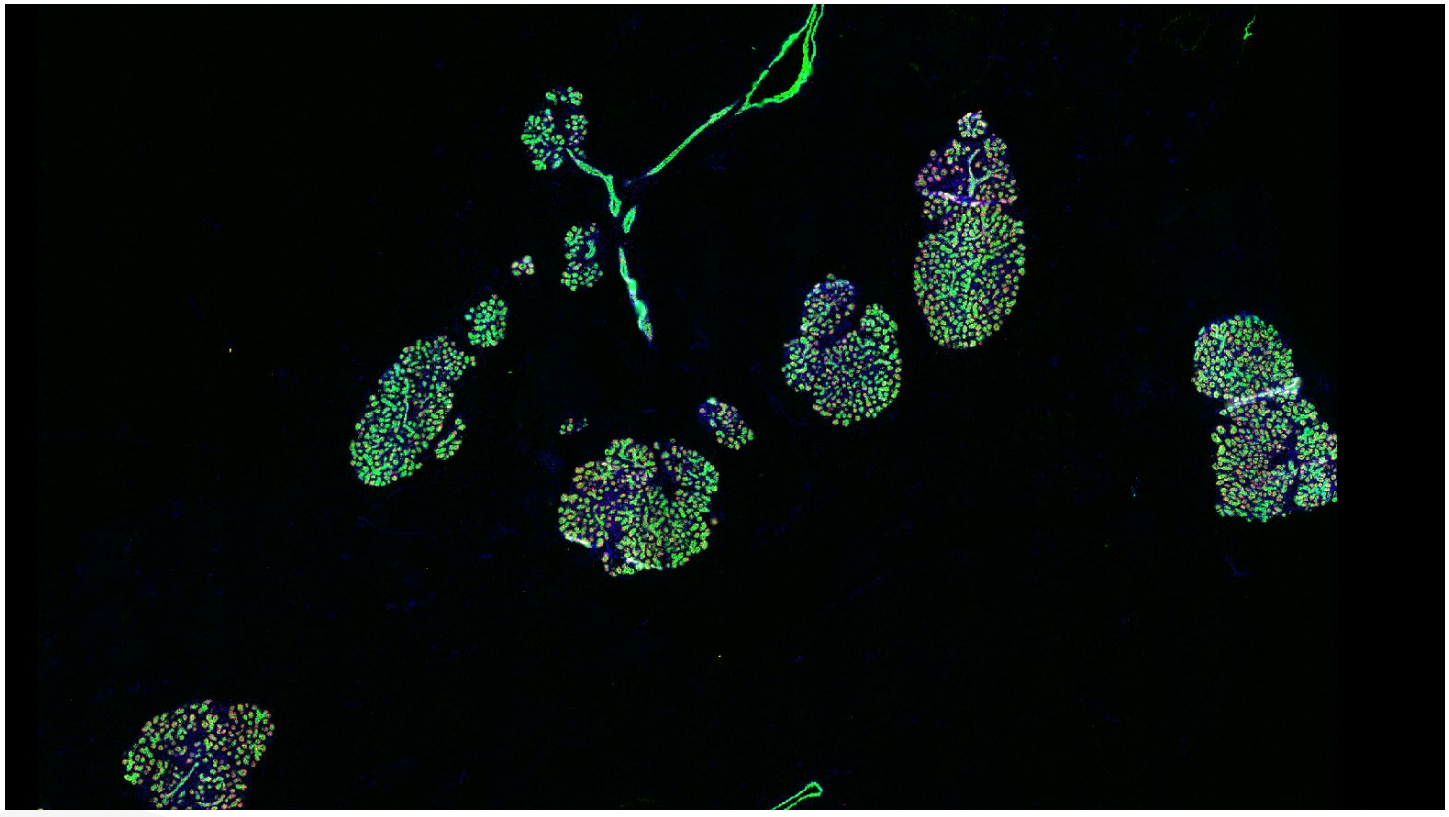

FIGURE 1:
By selecting for different label sets, a user can switch between particular areas of interest within the same sample. For instance, here DAPI and Keratin-19 label the secretory cells and ductwork within breast tissues without the surrounding tissue. Courtesy: Kessenbrock Lab, UC Irvine

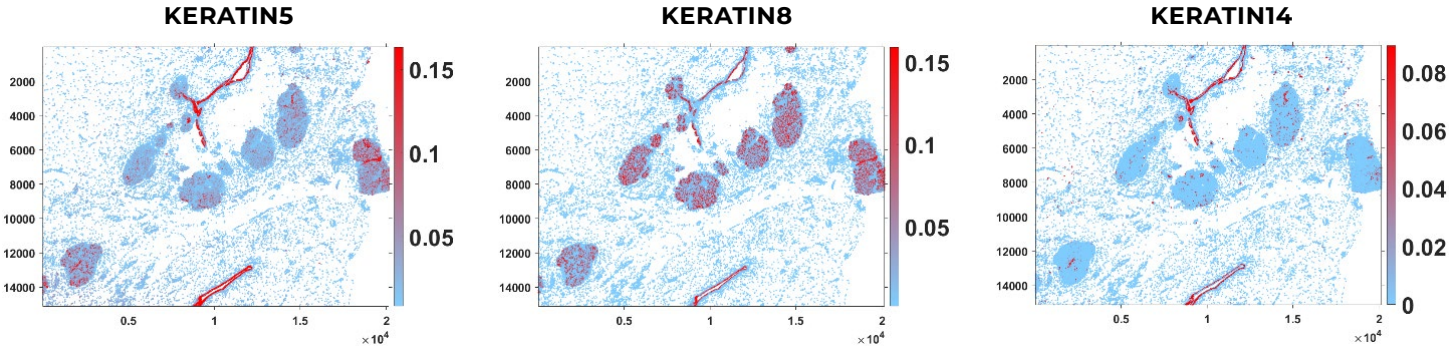

FIGURE 2:
Heat maps indicate the level of expression for each marker and where it is found in the tissue sample. Here, different expression patterns for Keratin-5, Keratin-8, and Keratin-14 point to different cellular phenotypes within a sample of healthy breast tissue.

Biomarker expression heat maps provide another perspective on this by showing labeling patterns across different cell clusters within the sample **(FIGURE 2)**. For instance, Keratin-5, -8, and -14 are all epithelial markers that are expressed in the breast tissue. Via this visualization, however, it is instantly apparent that these three, closely related molecules, have completely different spatial expression patterns, presumably due to their association with distinct cellular phenotypes.

For each of the labeled cell phenotypes, we can map how they cluster, and calculate which of the other cells they are most likely to interact with. Herein lies the power of spatial phenotyping and studying cellular function and behavior in context.

In this case, we used a Delaunay triangulation-based algorithm to map out patterns of neighboring cells to identify distinct cell-to-cell connections, and upon clustering and analyzing this data we could identify several 'cellular neighborhoods' with distinct clustering patterns.

FIGURE 3 lists each cell cluster by number along with the likelihood that any cell in the cluster will be surrounded by a particular cell phenotype. For example, in the graph on the left, we see that in Cluster 1 there's a roughly 40% likelihood that any given cell within the cluster will be adjacent to a CD4 T Cell. By comparison, we can see that within Cluster 8, there's a 60% likelihood that a given cell will be adjacent to a fibroblast.

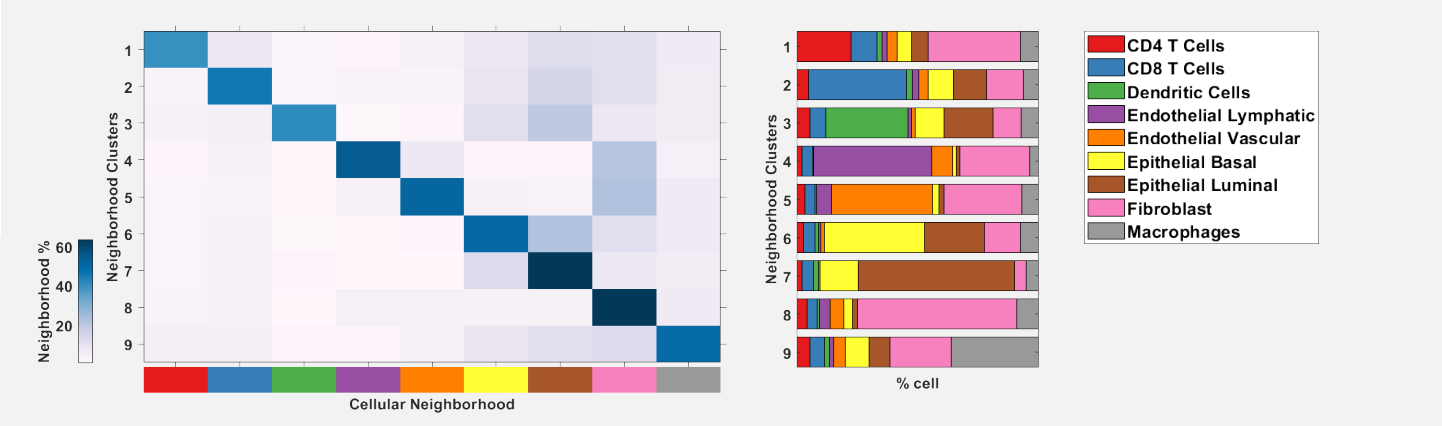

FIGURE 3:
This chart summarizes the nine predominant cell clusters in the sample and the likelihood that any cell in the cluster will be surrounded by a particular cell phenotype.

FIGURE 4 shows a map of actual cell proximity relative to our selected marker (CD4 in this case) in Clusters 1 and 2. In Cluster 1, the red CD4 cells are most likely to be proximal to other CD4 cells, followed closely by fibroblasts (in pink). In Cluster 2, CD4 cells are most likely to be adjacent to blue CD8+ cytotoxic T Cells. By contrast, in Cluster 6, CD4 cells are most likely to be adjacent to yellow basal epithelial cells, and in Cluster 7, they are most likely to be surrounded by epithelial luminal cells. Will a CD4 T Cell behave differently in each of these clusters? Each one of these associations is a distinct cellular niche with potentially different functional implications for the cell that is featured in the center of the diagram.

This just scratches the surface of the quality and scope of data that spatial phenotyping can reveal, yet it is difficult to look at these findings without forming new hypotheses about potential cell-to-cell interactions and their biological significance, and that's the point.

> Same cell, different context – that's the idea behind spatial phenotyping and how the microenvironment impacts disease progression and treatment response.

DR. AHMET COSKUN
Single Cell Biotech Lab, Georgia Tech

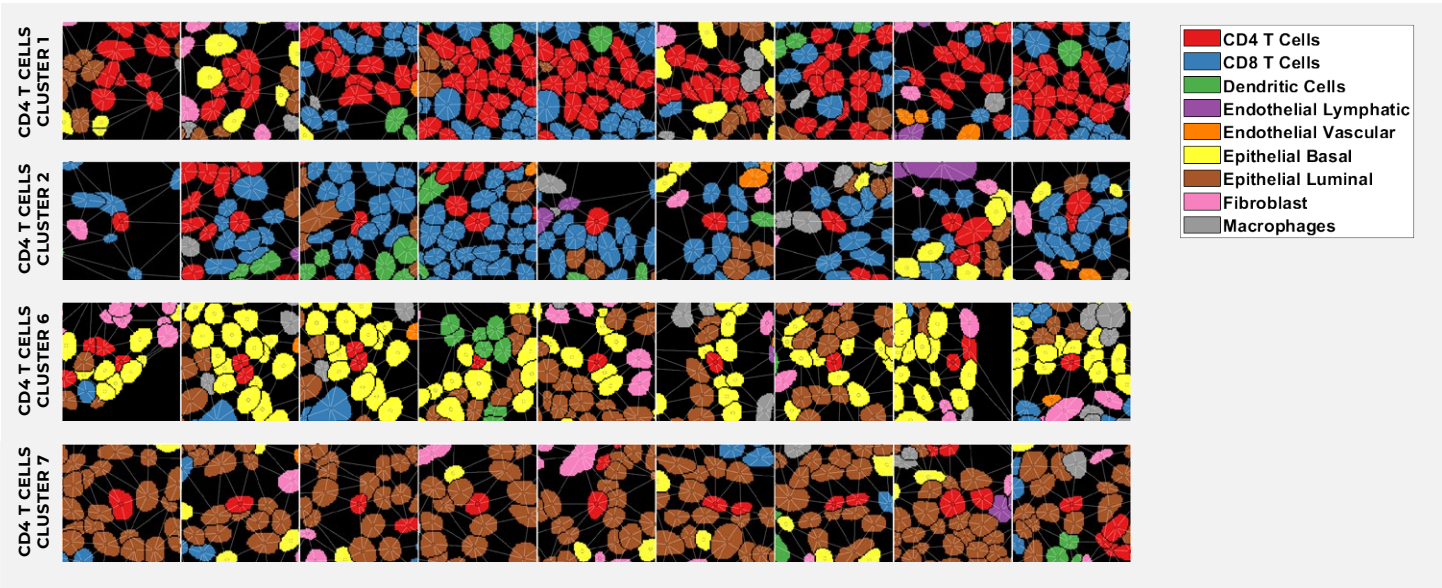

FIGURE 4:
Cluster maps show proximal relationships between different cell types within each cluster to highlight potential inhibitory or promotor relationships.

2 SEEING EVERY SINGLE CELL

One of the maxims of medical discovery in the 2020s is that the easy ones are all taken. We can't understand why patients with the same diagnosis respond differently to the same therapy, or why a mutation that is lethal in one patient is benign in another without questioning all of our assumptions and checking all the details.

In spatial phenotyping this starts with accounting for every cell in your sample. This may seem extreme when we consider that a typical tissue sample, the size of a capital M in this typeface, may contain hundreds of thousands or even a few million cells. Until now, though, most analytical approaches have assumed a certain level of homogeneity and accepted varying amounts of tissue loss as a routine aspect of sample preparation or handling.

> It's only when one actually sees and accounts for every cell in a sample that we can begin to appreciate all of the details that could be missed.

DR. OLIVER BRAUBACH
Head of Research Applications at Akoya Biosciences

In the example taken from a study of breast cancer FFPE tissue we see the predominance of epithelial tissue **(FIGURE 5)** marked by Keratin-5, Keratin-8, Keratin-18, Keratin-19, and collagen.

Yet with spatial phenotyping, that is just the start. We see here **(FIGURE 6)** that the system has registered all 63,056 distinct cells in this sample, each of which has an antibody and labeling value that is listed in a format akin to what you would see with scRNA-seq or flow cytometry. The difference is that each cell here also has an x-y coordinate to allow you to locate its exact location in the sample.

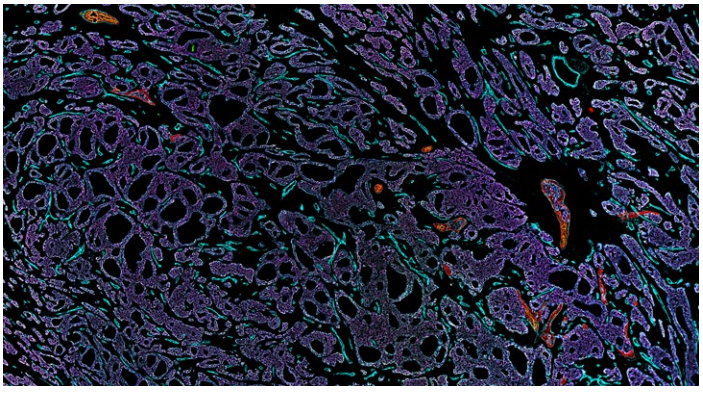

FIGURE 5:
This image of human breast cancer FFPE tissue (stained with a 36-plex antibody panel) is largely composed of luminal epithelial cells (purple) as well as basal epithelium (red).

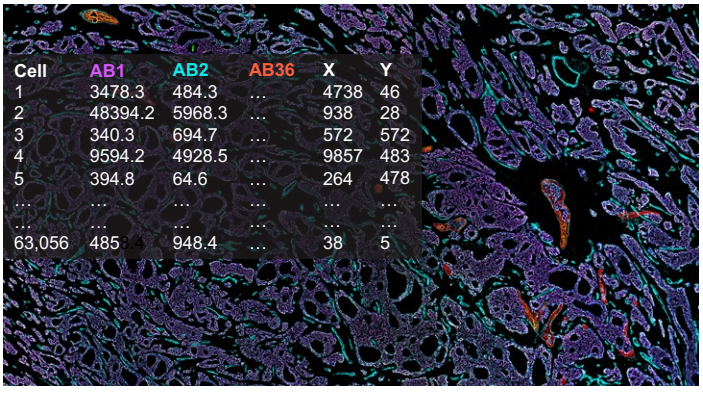

Cell	AB1	AB2	AB36	X	Y
1	3478.3	484.3	…	4738	46
2	48394.2	5968.3	…	938	28
3	340.3	694.7	…	572	572
4	9594.2	4928.5	…	9857	483
5	394.8	64.6	…	264	478
…	…	…	…	…	…
…	…	…	…	…	…
63,056	485	948.4	…	38	5

FIGURE 6:
The system indexes each cell and the degree to which it expresses each biomarker, and provides an x-y coordinate for locating the specific cell on the slide. The table here shows the first 5 of more than 63,000 cells.

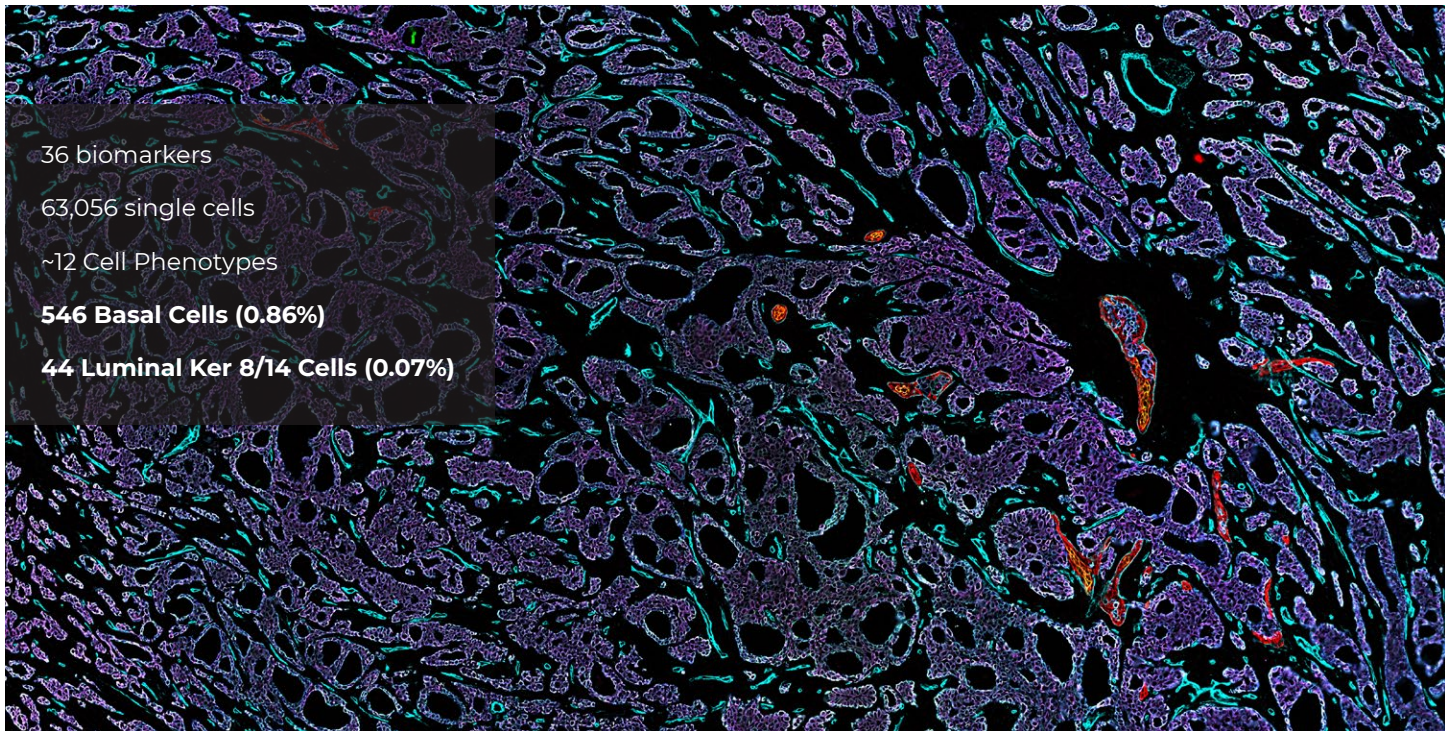

FIGURE 7:
Here we see how the system identified small clusters of distinct cells out of the tens of thousands analyzed. The 44 luminal cells labeled with Keratin-8 and -14 had only once before been observed in humans, and never before in pathogenic breast cancer tissue.

We can then use an unbiased clustering algorithm to identify and count each of the 12 different cell phenotypes that are present, and here amid the thousands of the expected basal and luminal cells, we see two extremely small and unexpected clusters **(FIGURE 7)**. In red we can see one unique cluster of 546 basal cells constituting less than 1% of all the cells in the sample.

Where we really see the value of single-cell resolution, though, is in this second cluster of luminal cells positive for Keratin-8 and -14. These are remarkable not just because of their extremely small number – just 44 out of 63,056 cells, or <0.1% of the total population – but also because they are of a type of epithelial cell previously only described in healthy breast tissue.[1]

We can learn more about each of these clusters in the expression profile table in **FIGURE 8**. The different markers are listed on the bottom of the heatmap with red indicating a higher expression level, while blue indicates little or no expression. Comparing the Luminal Keratin-8 /14 cells, we see that they also express TFAM and b-catenin more than basal cells. Basal cells, on the other hand, clearly stand out due to strong expression of TP63, a canonical basal cell marker.

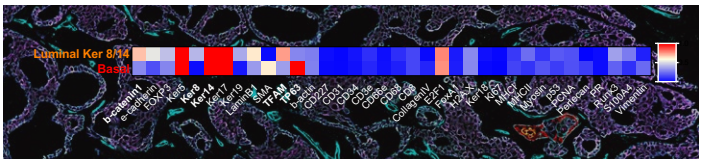

FIGURE 8:
An expression map for each cell type uses color to indicate levels of protein expression with red indicating high levels of expression and blue indicating no or low expression.

1. Nguyen QH, Profiling human breast epithelial cells using single cell RNA sequencing identifies cell diversity. DOI: NATURE COMMUNICATIONS | DOI: 10.1038/s41467-018-04334-1

Finally, just to confirm that these small numbers are not just analytical noise, we can return to the sample and locate each one in its original context **(FIGURE 9)**.

While research into the clinical relevance of these structures is still ongoing, the fact that they were revealed where they had never been seen before as part of an unrelated analysis underscores the value of single-cell resolution.

By comparison, lower-resolution methods or regions of interest-based (ROI) platforms create discontinuous spatial maps and lose the context of the larger sample, while some additionally omit much of the relevant data by ignoring regions that fall outside the ROI.

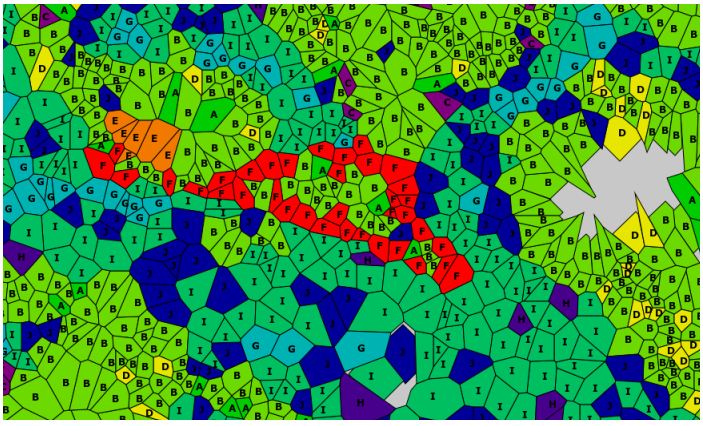

FIGURE 9:
A Voronoi representation of cell phenotypes, in a zoomed in region, shows the rare Luminal Ker 8/14 cells in orange (labeled as E), and the basal cells in red (labeled as F).

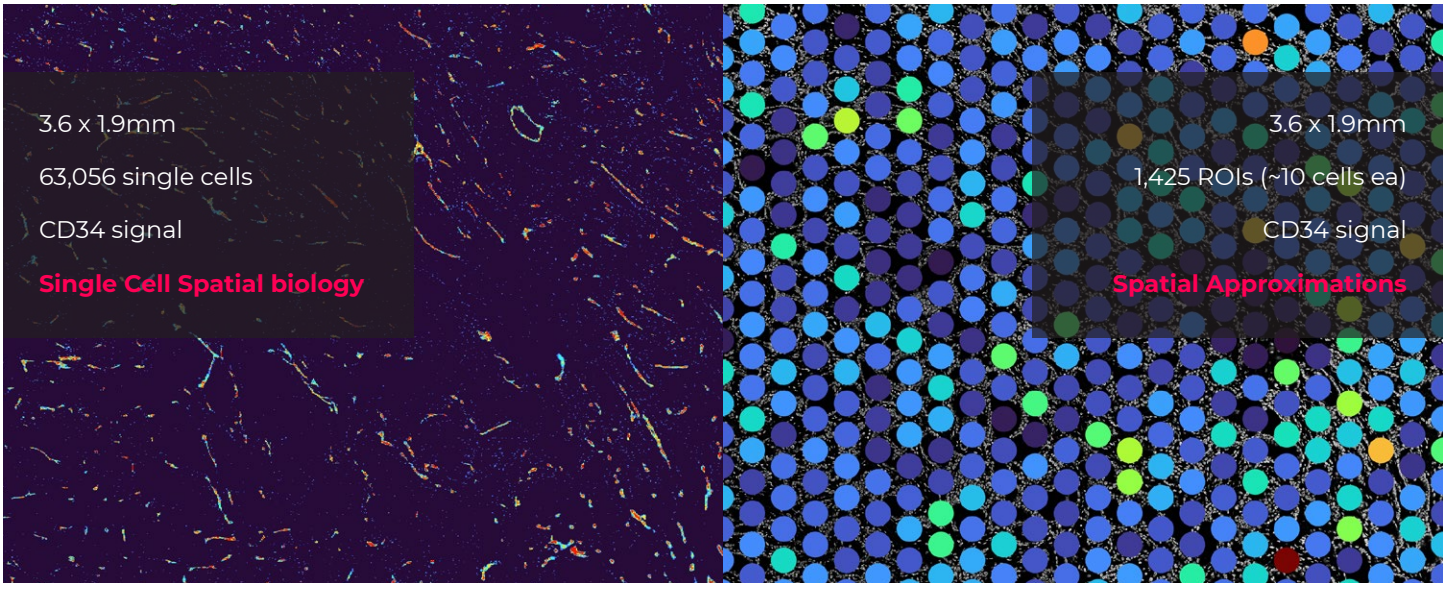

FIGURE 10:
Spatial phenotyping (left) shows individual cells in the context of the tissue, here revealing CD34 labeled vascular structures, compared to regional approximations with lower-resolution methods.

For instance, **FIGURE 10** compares two analyses of the same breast cancer tissue labeled with a blood vessel marker CD34. On the left, with single-cell spatial phenotyping, you can see the different long, short, and fat blood vessels that CD34 reveals, and you get a good sense of the vasculature and morphotype of this tissue section.

In this specific case, the 63,056 individual cells identified with spatial phenotyping are reduced to spatial approximations across just 1,425 ROI.

3

CELLULAR NEIGHBORHOODS: THE NEW PHENOTYPE

One result of seeing where every cell sits in the tissue labeled to reveal its specific function and phenotype is that patterns begin to emerge that align with particular pathologies or outcomes. Dr. Garry Nolan, a leading expert in spatial biology and Professor of Microbiology and Immunology at Stanford University, refers to these tissue structures as "cellular neighborhoods."

Nolan's lab demonstrated the utility of the neighborhood concept in colorectal cancer (CRC), where they sought to explain how the roles of different cell types change based on their position within the immune tumor microenvironment (iTME).

To do this, they identified two different CRC patient groups with significantly different prognostic outcomes. One cohort's iTME was characterized by numerous tertiary lymphoid structures (TLS) and labeled as CLR for "Crohns-like reaction." The group with the higher mortality rates was characterized by diffuse inflammatory infiltration (DII) but low TLS formation. It was labeled DII. For both groups, they used multiplexed tissue imaging to identify cellular neighborhoods (CNs) based on cellular composition and morphology **(FIGURE 11)**.

> The concept of neighborhoods quickly came to the fore, because we were seeing multiple groupings of cells that would repeat across a tissue, and these groupings would correlate with observations that pathologists have been making for 50 years.

DR. GARRY NOLAN
Professor of Microbiology and Immunology, Stanford University

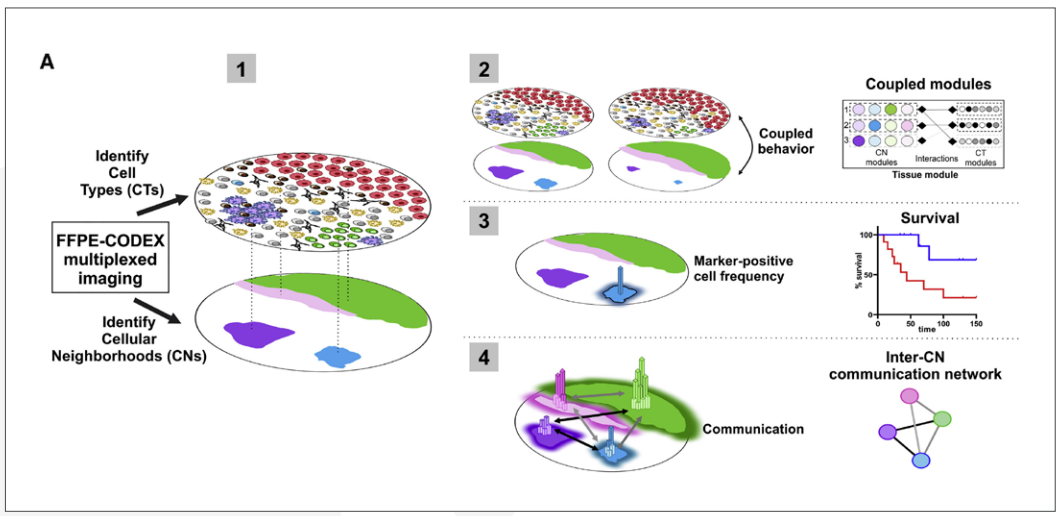

FIGURE 11:
Conceptual framework for CN mapping combining cell type as identified by label with the known composition and morphology of the tissue.
Source: Schürch, CM et al. Coordinated cellular neighborhoods orchestrate antitumoral immunity at the colorectal cancer invasive front. *Cell*. 2020 Sept 03; 182, p 1342. https://doi.org/10.1016/j.cell.2020.07.005

The hypothesis was that the difference in survival between the two groups was likely influenced by differences in their antitumoral immune response as opposed to tumor intrinsic factors, and this was borne out by the neighborhood mapping process.

The research focused on nine cellular neighborhoods that recapitulated core tissue components such as T-cell enriched (CN1), bulk tumor (CN2), macrophage enriched (CN4), tumor boundary (CN6), and granulocyte enriched (CN9) **(FIGURE 12)**. They found that the cellular composition of the different neighborhoods shifted between patients in the DII and CLR groups, and that disease prognosis in either group could be linked to specific intra-neighborhood interactions and changes in the cellular mix within neighborhoods.

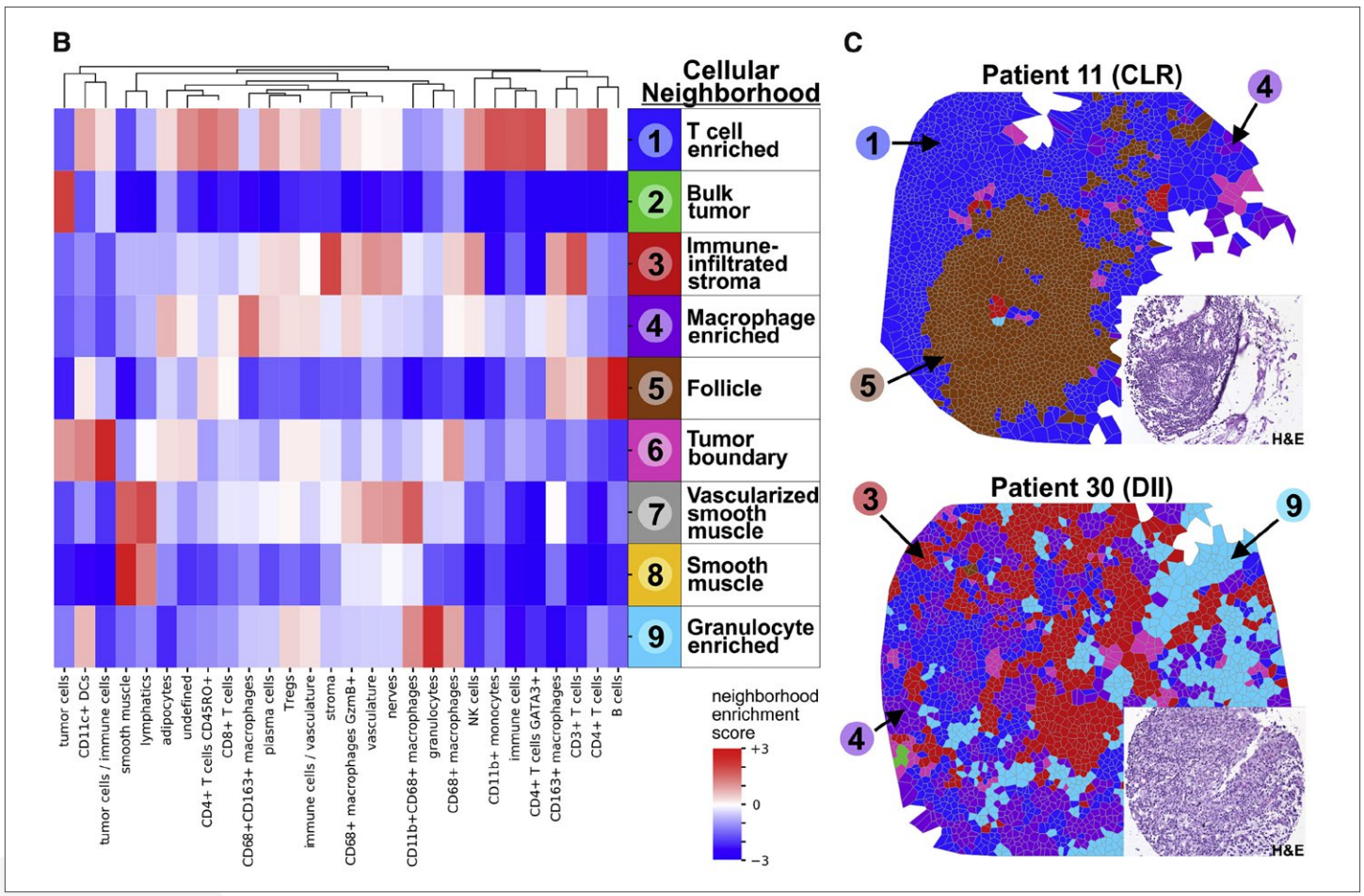

FIGURE 12:
Table B (left) lists the nine cellular neighborhoods identified in the colorectal cancer cells, and the cell types present in each. The maps on the right illustrate the difference in the relatively well-delineated neighborhoods in CLR patients and the highly intermixed neighborhood structures associated with poorer survival in DII patients.

Source: Schürch, CM et al. Coordinated cellular neighborhoods orchestrate antitumoral immunity at the colorectal cancer invasive front. *Cell*. 2020 Sept 03; 182, p 1348. https://doi.org/10.1016/j.cell.2020.07.005

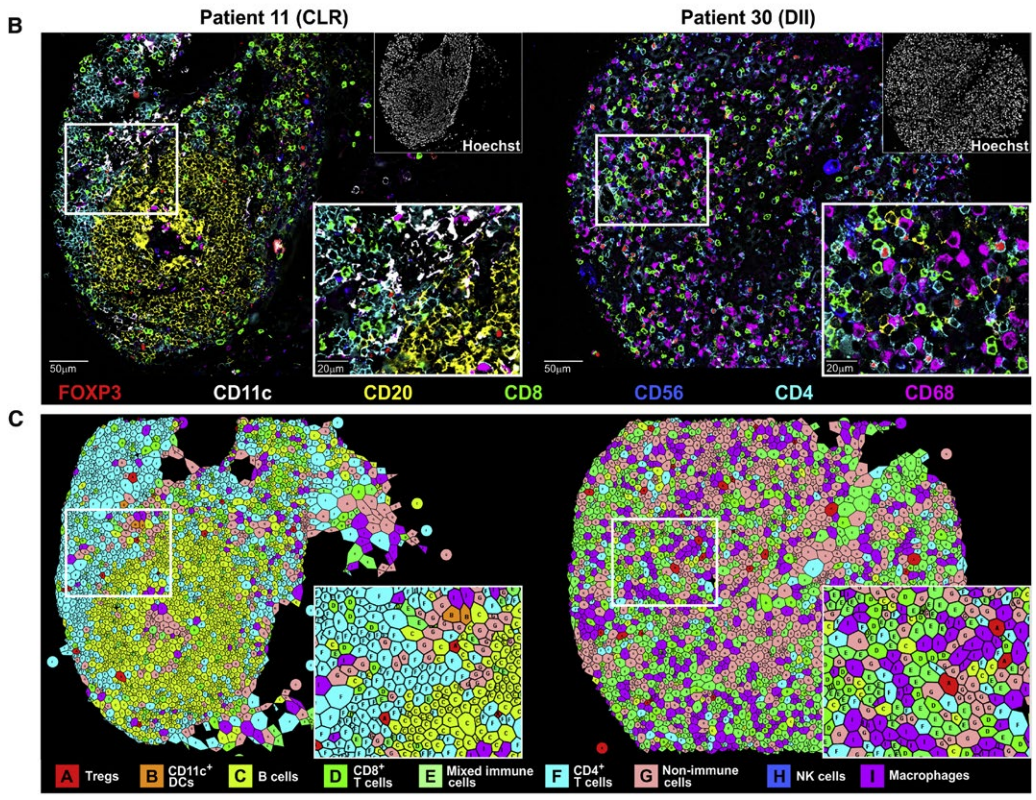

FIGURE 13:
Neighborhood structures in CLR patients are compartmentalized with a separate "tumor compartment" and "immune compartment," while in DII patients, tumor and immune compartments were mixed. The separate compartments correlate with a higher survival rate, suggesting that tumor cells may interfere with anti-tumor effects of immune cells in the mixed model.

Source: Schürch, CM et al. Coordinated cellular neighborhoods orchestrate antitumoral immunity at the colorectal cancer invasive front. *Cell*. 2020 Sept 03; 182, p 1346. https://doi.org/10.1016/j.cell.2020.07.005

In CLR patients the neighborhoods constituted a separate "immune compartment" and "tumor compartment," which correlated with higher survival rates **(FIGURE 13)**. By contrast, in DII patients the tumor and immune modules were combined in a single compartment, suggesting that in DII patients the tumor may interfere with or regulate anti-tumor immune processes. Notably, survival was higher in DII patients where there was a robust CD9 granulocyte neighborhood with elevated levels of PD-1+ and CD4+ T cells.

While these observations correlate with existing assumptions about the predictive value of TLS levels and CD4:CD8 ratios, this research for the first time showed how these relationships were tied to finer cell and protein interactions captured by the neighborhood model.

> It all comes back to a simple idea that the same immune cell placed in a different context within the tumor can play a completely different role.

DR. GARRY NOLAN
Professor of Microbiology and Immunology, Stanford University

Comprehensive Spatial Phenotyping with the CODEX® Ultra-High Plex Imaging Solution

All research referenced above was performed using the CODEX® platform.
For more details, visit www.akoyabio.com.

AKOYA BIOSCIENCES®
THE SPATIAL BIOLOGY COMPANY®